Journal of Environmental Radioactivity 214–215 (2020) 106172

Contents lists available at ScienceDirect

Journal of Environmental Radioactivity

journal homepage: http://www.elsevier.com/locate/jenvrad

Reconstruction of radiocesium levels in sediment off Fukushima: Simulation analysis of bioavailability using parameters derived from observed ^{137}Cs concentrations

Yutaka Tateda [a,*], Kazuhiro Misumi [a], Daisuke Tsumune [a], Michio Aoyama [b], Yasunori Hamajima [c], Jota Kanda [d], Takashi Ishimaru [d], Tatsuo Aono [e]

[a] Environmental Science Research Laboratory CRIEPI, Chiba, 270-1194, Japan
[b] University of Tsukuba, Ibaraki, 305-8577, Japan
[c] Kanazawa University, Kanazawa, 923-1224, Japan
[d] Tokyo University of Marine Science and Technology, Tokyo, 108-8477, Japan
[e] National Institute for Quantum and Radiological Science and Technology, Chiba, 263-8555, Japan

ARTICLE INFO

Keywords:
Radiocesium
Fukushima
Sediment
Numerical model
Bioavailability

ABSTRACT

Radiocesium was released to the North Pacific coastal waters by the accident at the Fukushima Dai-ichi Nuclear Power Plant (1FNPP) of the Tokyo Electric Power Company (TEPCO) in March 2011. Since the radiocesium in the sediment off Fukushima was suggested as a possible source for the transfer of this radionuclide through the benthic food chain, we conducted numerical simulations of ^{137}Cs in sediments off the Fukushima coast by using a model which incorporates dynamic transfer processes between seawater and the labile and refractory fractions in sediment particles. This model reproduced the measured temporal changes of ^{137}Cs concentration in seabed surface sediment off Fukusima coasts, by normalizing the radiocsium transfer between seawater and sediment according to the particle diameter sizes. We found that the ^{137}Cs level in sediment decreased by desorption during the first several months after the accident, followed by a reduction in the labile fraction until the end of 2012. The apparent decrease of the total radiocesium level in surface sediment was estimated to occur at rates of approximately 0.2 y^{-1} within a 20 km distance from the 1FNPP. The comparison of ^{137}Cs level decreases in the demersal fish and the simulated temporal labile fraction in fine sediment demonstrated that the consideration of radiocesium transfer via sediment is important for determining the ^{137}Cs depuration mechanism in some demersal fish.

1. Introduction

Radiocesium, ^{134}Cs (half-life 2.06 yr) and ^{137}Cs (half-life 30.2 yr), was released to the Pacific coastal waters by the accident of the Fukushima Dai-ichi Nuclear Power Plant (1FNPP) of the Tokyo Electric Power Company (TEPCO) on March 2011. From 0.1 to 2.0% of the radiocesium introduced into the coastal waters was adsorbed to the marine sediment off Miyagi, Fukushima, Ibaraki prefectures during 2011 (Kusakabe et al., 2013). After 2012, the ^{137}Cs concentrations in coastal shelf sediment off Fukushima decreased gradually (Otosaka, 2017; Kusakabe et al., 2017; Takata et al., 2017) and were similar within a 30 km radius distance from 1FNPP (NRA, 2019). The radiocesium in marine sediment particles was understood as being irreversibly bound by entering the clay mineral lattice (Fuller et al., 2015), however, the ^{137}Cs in sediment collected during 2011 was shown to be present in an organically bound fraction off Fukushima (Otosaka and Kobayashi, 2013; Ono et al., 2015). Since the radiocesium in the sediment off Fukushima was suggested as a possible source for the transfer of this nuclide through the benthic food chain (Wang et al., 2016; Tateda et al., 2016; Bezhenar et al., 2016), it is important to evaluate the bioavailable radiocesium concentration in bottom sediment following the Fukushima accident. For this estimation, it is also necessary to consider the particle size effect on the radiocesium level in sediments (Cundy and Croudace, 1995). This is because the ^{137}Cs activities in the sediments off

* Corresponding author.
E-mail addresses: tateda@criepi.denken.or.jp (Y. Tateda), misumi@criepi.denken.or.jp (K. Misumi), tsumune@criepi.denken.or.jp (D. Tsumune), michio.aoyama@ied.tsukuba.ac.jp (M. Aoyama), hamajima@se.kanazawa-u.ac.jp (Y. Hamajima), jkanda@kaiyodai.ac.jp (J. Kanda), ishimaru@kaiyodai.ac.jp (T. Ishimaru), aono.tatsuo@qst.go.jp (T. Aono).

https://doi.org/10.1016/j.jenvrad.2020.106172
Received 11 October 2019; Received in revised form 15 January 2020; Accepted 15 January 2020

Fukushima showed a spatially heterogeneous distribution being determined mainly by two factors. 1) the spatiotemporal variation of the ^{137}Cs activities in the overlying bottom water caused by point release from the source and higher deposition close to the 1FNPP than in the area far offshore; 2) the particle size composition in sediment in which the ^{137}Cs was adsorbed to a greater degree in sediment particles of smaller size (Ambe et al., 2014; Black and Buesseler, 2014; Misumi et al., 2014; Fukuda et al., 2018). Additionally, fine sediment particle resuspension and lateral transport to deeper regions was thought to be affecting the radiocesium levels in coastal sediment (Kusakabe et al., 2017).

In this study, we determined the dynamic transfer parameters of radiocesium between seawater and sediment particles of different size by the measured temporal ^{137}Cs concentrations in seawater and shore sediment collected during April to September 2011 in the southern Fukushima area. In the numerical model, we include the labile and refractory fraction of radiocesium content in sediment particles to reconstruct the changes in temporal levels during the initial period after the accident. After determining the dynamic transfer parameters for radiocesium between seawater and sediment, we calculated the temporal ^{137}Cs levels in sediment particles of different size by a numerical simulation model (Misumi et al., 2014). We verified the simulation results with the measured ^{137}Cs concentrations in bulk and fine sediment particles (<150 μm) collected at study sites and those found in benthos and the stomach contents of demersal fish. Then we reconstructed the temporal ^{137}Cs levels in bottom sediment at the monitoring stations of the TEPCO and the Fukushima Prefecture according to the particle size composition of both sites. Finally, we discuss the possibility of the labile fraction contribution to temporal changes of ^{137}Cs concentrations in the demersal fish reported by TEPCO (2019).

2. Material and methods

2.1. Sampling and measurement of field samples

2.1.1. Sediment collections for analyses

Four types of sediment samples were collected from the study site (Fig. 1). 1) Coastal shore sediment was collected from St. 4 to St. 6 during April 2011 to Sep. 2011. Sediment samples were freeze-dried and sieved through 1000, 600, 300, 150 and 38 μm mesh sizes of metal netting. 2) Seabed sediment was collected using a multiple core sampling device at St. A, B, C and IO2 during the Research Cruises UM-13-05 (Umitaka-maru) and SY-13-10 (Shinyo-maru) operated by Tokyo University of Marine Science and Technology during May and October 2013. 3) Seabed sediment was also collected using a core sampler (RIGO 5176) and Ekman bottom sampler (RIGO 5141) at T-S1, T-S8, T-S7 during 2013–2015. The top surface samples (0–1 cm) were freeze-dried and similarly sieved. 4) Sediment in the digestive system of benthos were collected by on board incubation (24–48 h, 6 °C) of heart urchin *Echinocardium cordatum* and sea cucumbers Molpadidae. The benthos samples were collected by a bottom dredge net from St. A, B, C, and IO2. Particle size of all of the samples were confirmed as <150 μm by sieving. 5) Sediment in the digestive system of demersal fish was separated from stomachs of the slime flounder *Microstomus achne* and marble flounder *Pleuronectes yokohamae*, in which the sediment amount was found in stomach as being significantly greater than those in olive flounder stomach (Fig. S1). The stomach samples of the above two demersal fish were provided by TEPCO from stations T-S1 to T-S8 after the fish were monitored for radionuclide levels. To evaluate the possibility of the contribution of sediment for radiocesium transfer to biota (Wang et al., 2016), several fine and bulk sediment samples were used to quantify the labile ^{137}Cs concentration by measuring the exchangeable fraction derived by extraction with 1M NH_4Cl followed by H_2O_2 digestion (modified method from Cundy and Croudace, 1995) as a bioavailable component which passes through the digestive tract.

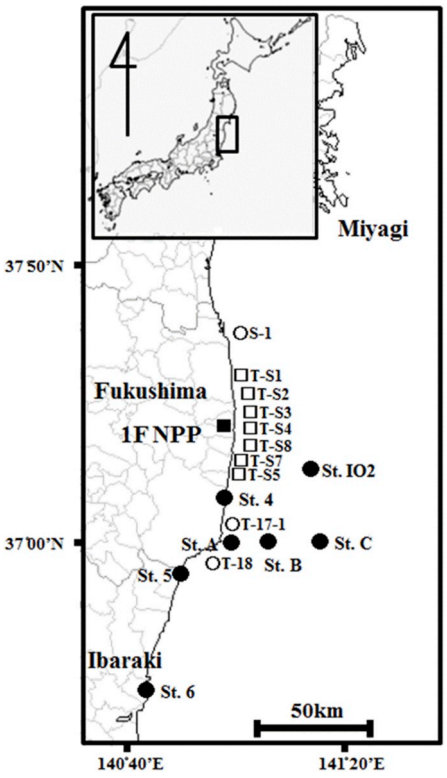

Fig. 1. Study sites (St) and the monitoring stations of TEPCO (T–S) and Fukushima Prefecture (S-, T-). Geographic coordinates of study sites are shown in Tables S2–S5.

2.1.2. Radiocesium analysis

The sediment samples were transferred to 100 ml polystyrene containers, and radioactive cesium was measured by gamma-spectrometry (Ge-detector GR2519, Inspector, 2000; CANBERRA). The counting efficiency of the sample was calibrated and determined using calibration software (ISOCS, Genie 2000; CANBERRA) and a set of standard gamma volume sources (MX033U8PP, JRIA). Radiocesium concentrations in the trace amounts of sediment in the digestive system of benthos, stomachs of demersal fish, and sieved fine sediment particles were analyzed in the underground ultra-low-level radioactivity measurement facility of Kanazawa University. Measurement times were adjusted to obtain a standard deviation from the counting statistics less than 5%.

2.2. Analysis by model simulation

2.2.1. Model and simulation

We used the dynamic model which has simulated the temporal ^{137}Cs activities in seabed sediment (Misumi et al., 2014). In this study, we newly defined the labile and refractory fraction of ^{137}Cs in our numerical calculations. The labile fraction is considered to be exchangeable mostly as the organic components on the surface of sediment particles, while the refractory fraction is assumed to be an irreversible component such as ^{137}Cs strongly bound in the clay mineral lattice of the sediment particle. Although we did not consider radiocesium 1) burial by bioturbation and 2) suspended particle settling/resuspension followed lateral transport in this model, these two contributions to the radiocesium amount in the surface sediment layer were elucidated with the apparent decrease rate ADR, which includes the above factors affecting the observed decrease rate of the total radiocesium concentration.

The prognostic equation for the ^{137}Cs activity in surface sediment is thus written as follows:

$$dC_{surf}(t)/dt = k^{surf}_1 C_{wat}(t) - k^{surf}_2 C_{surf}(t) - k^{inner}_1 C_{surf}(t) - \lambda C_{surf}(t) \quad (1)$$

$$dC_{inner}(t)/dt = k^{inner}_1 C_{surf}(t) - \lambda C_{inner}(t) \quad (2)$$

$$dC_{sed}(t)/dt = dC_{surf}(t)/dt + dC_{inner}(t)/dt \quad (3)$$

$$k^{surf}_1 = \chi S = \chi 3/(R \rho_s) \varphi (1 - p) \quad (4)$$

where $C_{surf}(t)$, $C_{inner}(t)$ and $C_{sed}(t)$ are ^{137}Cs activity in labile, refractory fractions and total content in sediment particles at time t (d), respectively; $C_{wat}(t)$ is activity in bottom seawater at time t (d); k^{surf}_1 and k^{surf}_2 (d^{-1}) respectively represent kinetic coefficients for adsorption onto and desorption from the surface of sediment particles off Fukushima by referring to the experimental values ((0.17–0.23)/(0.09–012) d^{-1} as adsorption/desorption rate constants Oughton et al., 1997; Rudjord et al., 2001); R is the radius of the sediment; ρ_s is sediment bulk density given as 1.7 g cm^{-3}, p is the porosity given as 0.6 (Misumi et al., 2014), and λ is the decay constant of ^{137}Cs. The kinetic coefficient k^{surf}_1 can be represented as the product of the exchange surface S with the exchange velocity χ given as 35 mm d^{-1} (Perianez, 2008). In this study, the adsorption and desorption rate k^{surf}_1 and k^{surf}_2 were finally determined from observed temporal ^{137}Cs concentration changes at St. 4 to 6 with fitting the simulated levels by a least squares method using a dimensionless correction factor φ (0.01, 0.03, and 0.15 for St.4, 5, and 6, respectively, (Perianez, 2008; Misumi et al., 2014). The phase exchange rate constant k^{inner}_1 0.0003 d^{-1} was determined by the experimental values ranging from 0.0003 to 0.001 d^{-1} (Rudjord et al., 2001) with fitting the resultant ratio of $C_{surf}(t)/C_{sed}(t)$ to the reported temporal ratio of exchangeable fraction (20% by Otosaka and Kobayashi (2013) for 2011 and 1–14% by Ono et al. (2015) for 2015). In the simulations, $C_{wat}(t)$ was externally set and C_{sed} was obtained by solving Equations (1) and (2). Using the data of Aoyagi and Igarashi (1999) and Ambe et al. (2014), the median particle diameters of surface sediment at each grid in the simulated area were determined.

We simulated the ^{137}Cs activities in the surface sediment layer off the Fukushima coast from 1 March 2011 to 30 September 2018 by using the simulated ^{137}Cs activities in bottom waters (C_{wat}) generated by the ROMS model (Tsumune et al., 2012, 2013) and solving Equations (1) and (2). The horizontal resolution of both the sediment and ocean models was 1 km. Initial ^{137}Cs activity in the surface sediment was assumed to be 1.0 Bq kg^{-1} (NRA, 2019). The ^{137}Cs input assumed a scenario for direct release that started on 26 March 2011, followed by the different release rate curves until September 2018.

2.2.2. Published data sets of seawater, sediment and demersal fish

For verification of the simulated result of the ^{137}Cs concentrations in bottom seawater and surface sediment from stations T-S1 to T-S8 within 20 km distance from 1FNPP (TEPCO, 2019), the data reported by NRA (2019) during May 2012 to August 2017 and February 2012 to September 2018, respectively were used. Among TEPCO monitoring stations, the data number of T-S2 was not sufficient to cover the study period 2011–2018, thus they were not used. Concerning the early period 2011–2012, the data were only collected outside of 30 km radius area, therefore we verified the simulation result by using the observed ^{137}Cs concentration in sediment at three monitoring stations (Fukushima Prefecture, 2018) in which the data for seawater and sediment were compiled for the northern (S-1) and southern (T-17-1, T-18) stations off Fukushima (Fig. 1). To complement the data for ^{137}Cs concentration in fine particle and bulk surface sediment, the reported data for T-S8, T-S7 (Ono et al., 2015), St. A, B, C, IO2 (Fukuda et al., 2018) were also used. The reported monitoring data for the ^{137}Cs concentrations in muscle of the demersal fish slime flounder, *Microstomus achne* (TEPCO, 2019), were used for the correlation analysis comparing those data with the radiocesium concentrations in the sediment.

3. Results

3.1. Temporal change of ^{137}Cs concentration in shore sediment particles of different size

The ^{137}Cs concentrations in shore sediment particles of different diameter sizes at St. 4 to St. 6 (Table S1) are shown in Fig. 2. The ^{137}Cs concentrations in bulk samples (Table S2) are also shown. The ^{137}Cs concentrations in bulk sediment at shore stations in southern Fukushima were elevated to approximately 1k Bq kg-dry^{-1} at St. 4 and St. 5. In contrast, at St. 6 the measured concentration was a maximum at approximately 30 Bq kg-dry^{-1}. Concerning the ^{137}Cs activity in sediment particles of different size, the concentration increased from approximately 1k to 100k, 1k to 10k Bq kg-dry^{-1} associated with a particle diameter size decrease from 1 mm to 0.019 mm at St. 4 and St. 5, respectively. The radioactivity increase with a decrease in particle size from several tens to 100 Bq kg-dry^{-1} was also evident at St. 6.

The temporal changes of the ^{137}Cs radioactivity in sediment particles were reconstructed with simulation by solving equations (1)–(4), using the calculated seawater levels (Fig. S2) derived by ROMS (Tsumune et al., 2012, 2013). The simulated levels in sediment, derived by the normalization of radiocesium transfer with particle size, was verified by the measured concentration in particle of each size at three stations. The result verified the model capacity to generate valid result ($r^2 = 0.84$, $p < 0.01$, XLSTAT, Fig. S3). The simulated level demonstrated that the maximum ^{137}Cs activity in sediment particles of 0.019 mm diameter at St. 6 was approximately 1k Bq kg-dry^{-1} at locations where the quantity of sample was not sufficient to obtain the measured concentration. For the bulk sediment, the temporal changes of the measured ^{137}Cs concentrations at St. 4 to 6 were almost explainable by the simulated radiocesium levels using a median particle size as the observed values of 0.9, 0.4, and 0.8 mm for the St. 4, St. 5, and St.6, respectively, according to the grain size compositions.

3.2. Measured ^{137}Cs concentrations and the simulated levels in sediment particles off Fukushima

The relation of the simulated ^{137}Cs levels in bottom sediment and the measured temporal ^{137}Cs concentrations in bulk surface sediment of all studied sites (St A, B, C and IO2, Table S3) and the observed concentrations (T-S1, T-S3 to T-S8, T-S7, T-S5, S-1, T-17-1, T-18) are shown in Fig. 3-a). The simulated and the measured ^{137}Cs concentrations in fine particles (diameter < 150 μm) are also shown in Fig. 3-b). The simulated result derived with median particle size of each studied station reproduced the observed ^{137}Cs concentration of bulk surface sediment sufficiently ($p < 0.001$), while the observed levels exhibited wide variation compared to the simulated level, resulting in the determination coefficient of $r^2 = 0.52$. The result of fine particle was similar in that the correlation between the simulated level and the measured concentration was significant ($p < 0.001$), however the determination coefficient ($r^2 = 0.32$) was smaller than that for the result of bulk sediment. In general, the simulated temporal levels in bulk surface sediment were compatible with the observed ^{137}Cs concentrations in collected surface sediment. The simulated levels for fine particles were comparable with the measured concentrations in fine sediment particles, while demonstrating larger variation.

The ^{137}Cs concentrations in sediment found in digestive system of benthos (Table S4) and demersal fish (Table S5) were evaluated as not being significantly different from the ^{137}Cs concentration in the fine particles of bottom surface sediment (Table S3)(*t*-test, EXSTAT), hence, those were considered as compatible to the fine bottom sediment.

Temporal ^{137}Cs levels over time during 2011–2018 in bulk bottom surface sediment reconstructed at the TEPCO monitoring stations are shown in Fig. 4-a), and those from north and south of Fukushima Prefecture (S-1, T-17-1, and T-18) are shown in Fig. 4-b). The simulated result demonstrated that the ^{137}Cs levels in the surface layer of the sea-

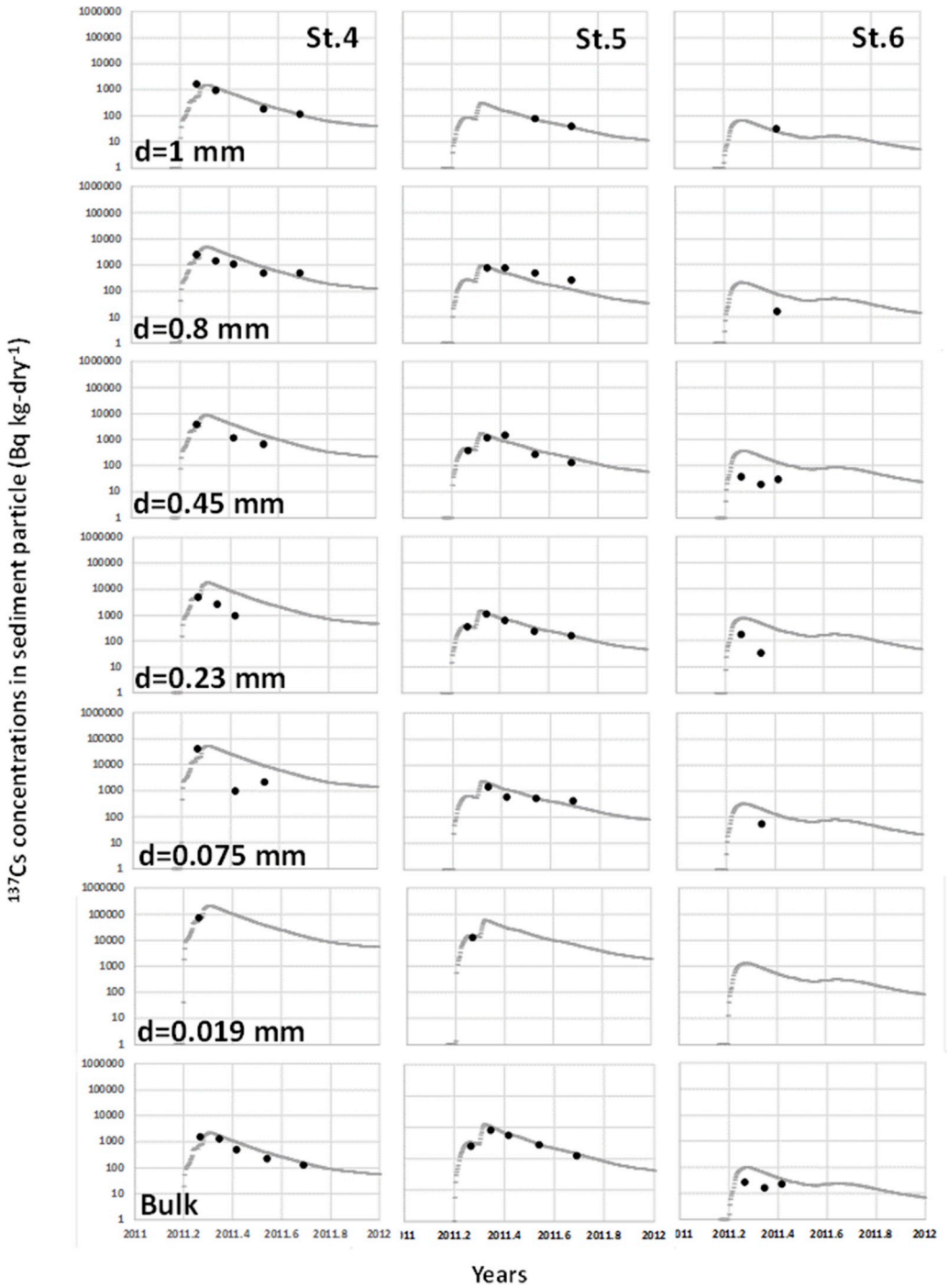

Fig. 2. Measured ^{137}Cs concentrations (●) over time in shore sediment particles of different diameters size and bulk sediment at St. 4 to St. 6 shown with the simulated levels (gray dotted lines).

bed along the Fukushima coastal area increased from 10 Bq kg-dry^{-1} to 1000 Bq kg-dry^{-1} during 2011 following the slow decrease to 10 Bq kg-dry^{-1} until 2018. The simulated level during 2011 was confirmed, since the assessment including the most dynamic period resulted in a good agreement with the observed temporal ^{137}Cs concentrations ($p < 0.001$) from the data collected during 2011 (S-1, T-17-1, T-18).

The apparent depuration rate (ADR) of ^{137}Cs concentration in bottom sediment within a 20 km radius area of the TEPCO monitoring stations, was derived by fitting the simulated decrease ratio to observed temporal change by a least square method with 95% confidence limit (Fig. S4). The derived ADRs were 0.23, 0.39, 0.12 and 0.20 y^{-1} at T-S3 ($p < 0.001$), T-S4 ($p < 0.001$), T-S7 ($p < 0.01$), and T-S5 ($p < 0.05$), respectively. For the reference, the ADR for T-S1 and T-S8 were calculated as 0.07 and 0.19 y^{-1} ($p > 0.05$).

3.3. Simulated ^{137}Cs levels of labile and refractory fractions in fine sediment particles

The simulated total ^{137}Cs levels in fine sediment with those in the labile and the refractory fraction at TEPCO monitoring stations are shown in Fig. 5. The measured ^{137}Cs concentrations in 1) sediment from the surface layer, 2) those found in the stomach contents of slime flounder collected at each of the monitoring stations are shown as analogues, and 3) concentration derived as the exchangeable fraction, are

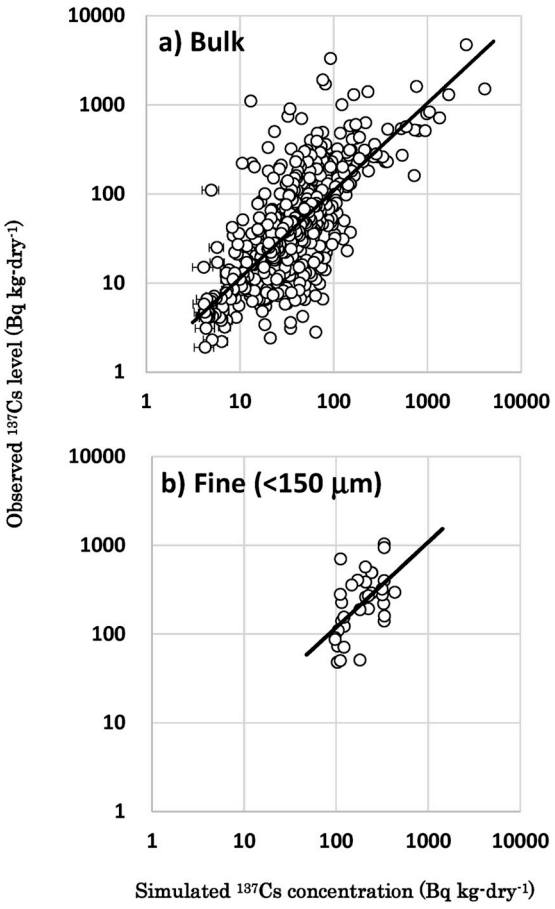

Fig. 3. a) Relation of the simulated ^{137}Cs levels in surface sediment and the measured and observed ^{137}Cs concentrations in bottom surface sediment (○) with the correlation curve (solid line). b) Relation of the simulated ^{137}Cs levels in fine sediment (particle size 75 μm) and the measured ^{137}Cs concentrations in fine sediment particles (<150 μm) in bottom surface sediment (○) with the correlation curve (solid line).

also shown. The reported concentration of the ^{137}Cs in fine particles and the exchangeable organic fraction reported by Ono et al. (2015) are additionally shown. The measured ^{137}Cs concentrations for fine surface sediment particles during 2013 were higher (100–1000Bq kg-dry^{-1}) at T-S3, T-S4 and T-S8 in the water near the 1FNPP, than those (10–100 Bq kg-dry^{-1}) at T-S1, T-S7, and T-S5 north and south of the 1FNPP. Simulated ^{137}Cs levels in the fine particles decreased gradually, and those were comparable with the measured temporal ^{137}Cs concentrations at T-S8 and T-S7, and with the reported values (Ono et al., 2015). Overall temporal change trend was similar to the decrease of radiocesium levels in the bulk surface sediment as shown in Fig. 4-a). The simulated ^{137}Cs levels in refractory fractions were evaluated to increase during the first year, and were estimated as being the dominant fraction in the total radiocesium content of fine particles after 2012.

Concerning the ^{137}Cs concentrations in the exchangeable fraction, the measured concentrations in sediment of T-S1 and T-S8 were higher than the simulated levels, whereas they were comparable with the observed concentrations at T-S8 (Ono et al., 2015) during 2012. The simulated ^{137}Cs levels in the labile fraction in fine particles were evaluated as rapidly decreasing by approximately two orders of magnitude until 2012, while exhibiting a slower decrease between 2013 and 2018 than occurred from 2011 to 2012. The calculated ratios of labile fraction to the total ^{137}Cs level in sediment from monitoring stations (Tables S3 and S4), and the ratio from the reported values were within a range of 0.01–0.25, which were comparable with the temporal ratio derived from simulation in this study (Fig. S5).

3.4. Relation of ^{137}Cs concentration in demersal fish and sediment

The relation of the temporal changes of the ^{137}Cs concentrations in 1) bulk surface sediment, 2) muscle of slime founder, associated with 3) the simulated ^{137}Cs levels in the labile fraction at T-S1, T-S3, T-S8, T-S7, T-S5 are shown in Fig. 6. The fitting curves for each decreased ratio of the above three cases are also shown. Analysis of correlation of the temporal decrease ratio of ^{137}Cs concentrations between the demersal fish and the labile fraction in sediment were significant ($r^2 = 0.54$–0.81, $P < 0.001$) at all of the above TEPCO monitoring stations. In contrast, those between the ^{137}Cs concentration in bulk sediment and in fish were not correlated ($p > 0.05$).

4. Discussion

The dynamic transfer parameters for radiocesium between seawater and sediment particles were determined in this study, derived by the measured temporal changes of the ^{137}Cs concentrations in seawater and shore sediment particles which were measured along southern coast of the 1FNPP during the six months after the accident. The dynamic radiocesium transfer parameters were identical to those which have been previously reported (Oughton et al., 1997; Rudjord et al., 2001; Perianez, 2008; Misumi et al., 2014), and the derived adsorption rate constant was confirmed to be applicable to the bottom sediment particles of the coastal area within 20 km distance from the 1FNPP. In contrast, the labile (exchangeable) fraction ratio was initially given as 1.0 in this study, compared to the organic fraction fixed ratio of 0.2 in the previous two year's evaluation for the radiocesium inventory in the sea-bed off Fukushima (Misumi et al., 2014). Therefore, the results demonstrate that the desorption of radiocesium from sediment was generated as being more rapid during several months (Figs. 2 and Fig. 4-a), b)) than those reported for the area outside of the 20 km radius from the 1FNPP (Misumi et al., 2014). Reconstructed rapid depuration of radiocesium from sediment during the initial phase is understood as being desorption from sediment particles as a result of the rapid decrease of radiocesium activity in seawater (Fig. S6).

After late 2011, the simulated refractory fraction was evaluated as being dominant in the radiocesium content of the sediment particles (Fig. 5), because the labile fraction decreased gradually which resulted in the decreasing rate of depuration of the ^{137}Cs content from bulk sediment as observed in Fig. 4-a), b). In this study, the refractory fraction required approximately a half year to become dominant. This result from the offshore Fukushima sediments agreed with the laboratory result using ^{134}Cs tracer in seawater and sediment in an experimental tank (Oughton et al., 1997), and believed to be as aging effect which determines the chemical form of radiocesium in the sediment layer.

After the refractory fraction became dominant, the ADR was derived for understanding the observed slow decrease of radiocesium content in sediment after 2012. Among the selected stations, there was considerable variation of the observed ^{137}Cs concentrations in bulk sediment after 2012, e.g. T-S3, T-S4, T-S5. One possible factor believed to cause the variation was the heterogeneity of radiocesium distribution in the sea-floor off Fukushima which was noted to be related to the fine scale topography, e.g. location of the mud deposition area (Thornton et al., 2013). Thus, the observed variation could be caused by heterogenous distribution of fine sediment within a monitoring station. In addition, ^{137}Cs-enriched particle (CsEP) were found in sediment (Ikenoue et al., 2018) which had possibility to elevate the observed high concentration anomalies. Though the observed variation may be affected by the above mentioned factors, the derived ADRs as a range of 0.12–0.39 y^{-1} confirmed the radiocesium removal by approximately 20% annually from the surface layer of the coastal sea-bed of Fukushima. Since the bottom sediment in the studied area are sandy (median grain sizes:0.13 to 0.46, Ambe et al., 2014), the resuspension and seaward transport of fine particles (Kusakabe et al., 2017) is considerable and is a possible driving factor. Another possibility is bioturbated vertical mixing

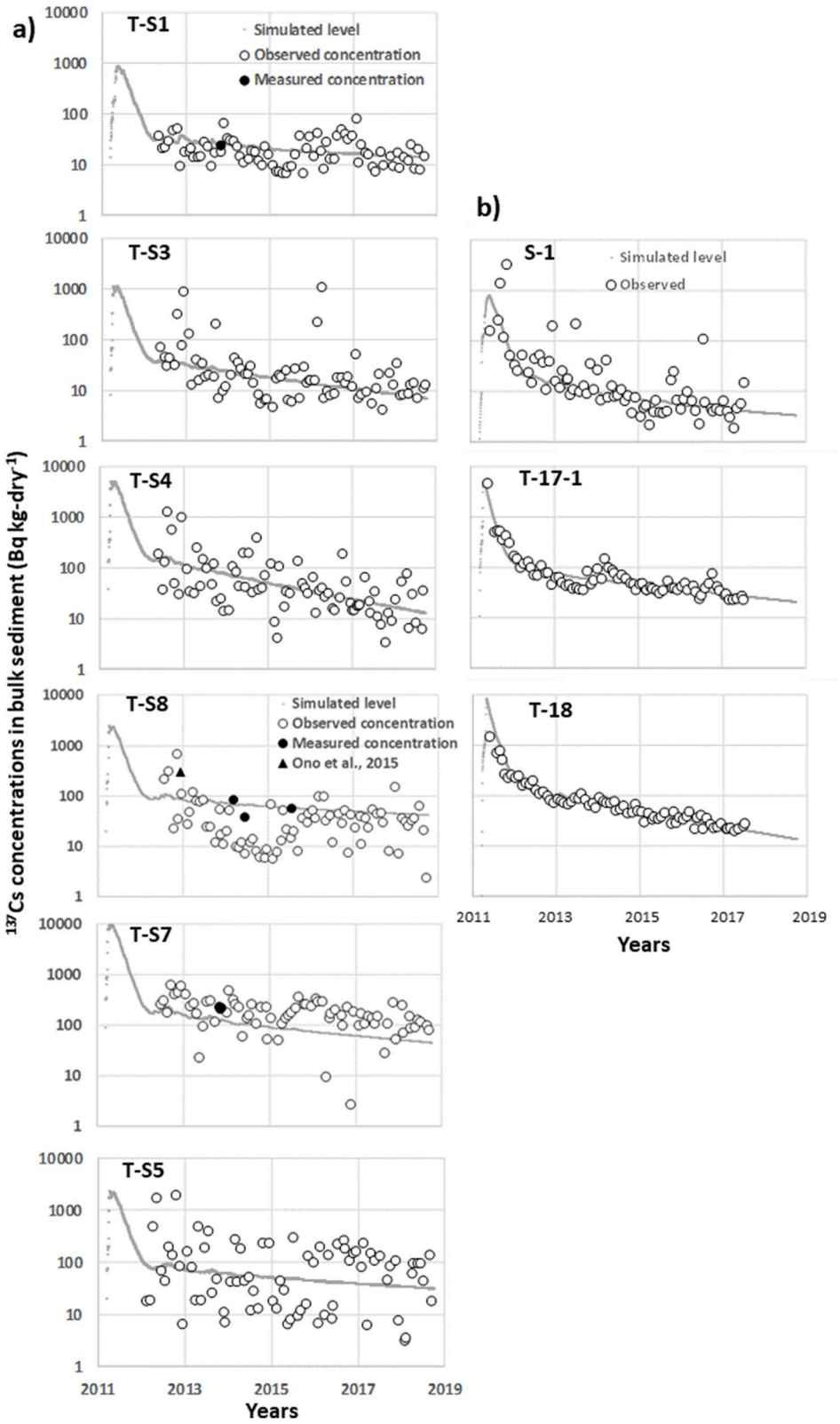

Fig. 4. a) Simulated (gray solid line) and observed ^{137}Cs concentrations (○) and the measured concentrations in this study (●) over time in bulk surface sediment at TEPCO monitoring stations (T-S1 to T-S8) during 2011–2019. The reported concentration (▲) is also shown. b) Simulated (gray solid line) and observed ^{137}Cs concentrations (○) over time in bulk surface sediment at Fukushima Prefecture monitoring stations (S-1, T-17-1, T-18) during 2011–2018.

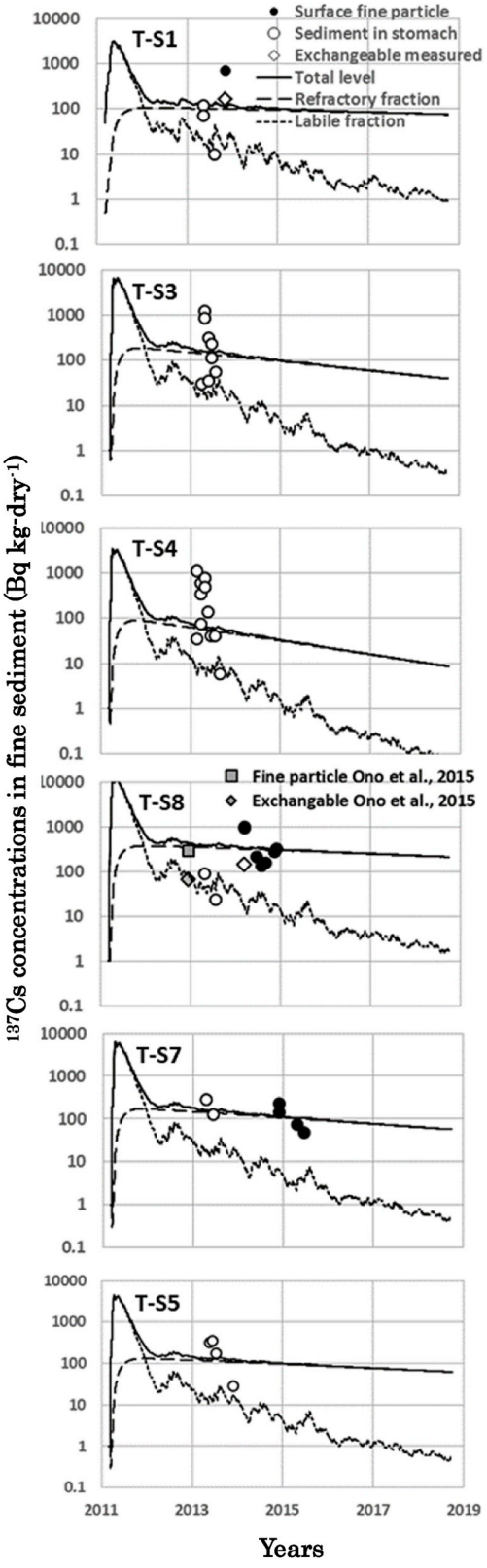

Fig. 5. Temporal variations in the simulated total (solid line), refractory (broken line), labile (dotted line) ^{137}Cs levels in fine sediment (particle diameter size 75 μm) with the measured ^{137}Cs concentrations (○) in sediment in the stomach contents of demersal fish, the surface fine sediment (●), exchangeable fraction (⋄). The reported concentration in fine sediment (▣) and in the exchangeable fraction (◈) are also shown.

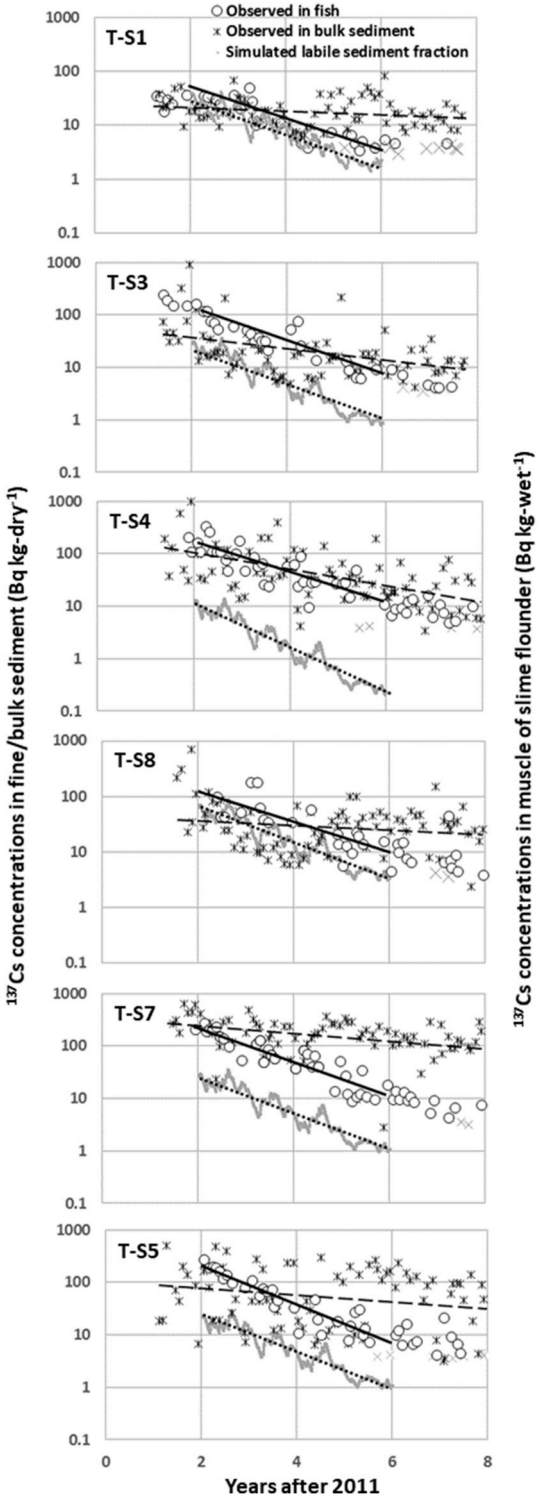

Fig. 6. Observed ^{137}Cs concentration in muscle of slime flounder (○) and the simulated labile fraction (gray line) with the measured ^{137}Cs concentrations in bulk sediment (⁎) at TEPCO monitoring stations during 8 years after 2011. The approximated curves are shown for the data (fish: solid line, sediment: broken line, labile fraction: dotted line) during 2013–2016 to avoid fitting error which originated from the reported below detection level cases in fish after 2017.

between surface and deeper sediment layers as observed at some nearshore sampling stations (Otosaka et al., 2014; Otosaka, 2017; Fukuda et al., 2018). Since the sediment composition is stable, therefore a plausible mechanism to compensate for the possibility of transported

fine particles in the coastal seabed is suggested to originate from a supply of discharged fine particles from rivers, an occurrence that was noted in the northern portion of the Fukushima area (Nagao et al., 2013). After the concentration in the initially contaminated sediment was decreased, the introduction of terrigenous particles with high radiocesium contents may become a possible delay factor in affecting radiocesium inventory changes in these coastal bottom sediments in the future.

Concerning the labile radiocesium fraction in sediment, it is important because of its effect on the radionuclide bioavailability and subsequent transfer via active sediment ingestion by some demersal fish e.g. slime founder. Since the fine sediment particle layer is known to be rich in organic matter (<5%, Ambe et al., 2014) with a comparatively larger radiocesium content (<20%, Otosaka and Kobayashi, 2013; Ono et al., 2015), the fine particle contribution to the radiocesium transfer through the benthic food chain can be substantial (Wang et al., 2016; Tateda et al., 2016). In this study, the ratio of the exchangeable ^{137}Cs concentrations in sediment were found to be within a range of 0.05–0.23 during 2013–2015. By the simulation, the labile fraction is evaluated as decreasing and is understood to be finally converted to a refractory fraction (Cundy and Croudace, 1995; Oughton et al., 1997). Assuming the labile radiocesium fraction in sediment is bioavailable, the compatibility of the measured ^{137}Cs concentrations in fine sediment found in the digestive system in benthos and demersal fish, with those in fine surface sediment (Fig. 5), suggests that this pathway as being is substantial for the delay of radiocesium depuration in active sediment feeding demersal fish. The positive correlation between the time series data of the ^{137}Cs concentrations in the muscle of slime flounder and the labile fraction level in fine sediment (Fig. 6), supports the contribution of a bioavailable fraction of ^{137}Cs in the sediment. If the exchangeable radiocesium ratio remained stable ratio e.g. 0.1, being an analogue to the radiocesium level in bulk sediment, the radiocesium depuration in slime flounder should be similar to the ^{137}Cs decrease ratio in bulk sediment. However, it was shown that the depuration curves were not comparable with those of the total ^{137}Cs concentrations in bulk surface sediment. Therefore, the labile radiocesium fraction in sediment as shown in Fig. 5 is equally important in playing some role in affecting radiocesium depuration from demersal fish off Fukushima.

Concerning the other controlling factors, such as seawater and prey organisms, the ^{137}Cs transfer from seawater to fish is not thought to be substantial after 2013 (Ishimaru et al., 2019) even in fish inhabiting waters close to the 1FNPP. In contrast, the transfer coefficient of radiocesium from sediment to benthic polychaetes was evaluated as <0.03 (Ono et al., 2015) and some radioactivity was retained in polychaetes after sediment ingestion (Shigenobu et al., 2015). Therefore, the bioavailable radiocesium in prey organisms has to be assessed through a detailed analysis of the radiocesium content in soft parts and detritus. In particular, the radiocecium transfer from radiocesium-rich interstitial water to detritus and benthos is considered as being potentially important.

The radiocesium transfer through the ingestion of benthic organisms by demersal fish is not yet well clarified. To obtain a through understanding of this transfer process, further study is needed to identify the mechanisms determining radiocesium levels in demersal fish by making a quantitative comparison of radionuclide transfer via both benthos ingestion and entrained sediment.

5. Conclusion

We conducted numerical simulations of ^{137}Cs concentrations in sediments off the Fukushima coast by using a model which incorporates dynamic adsorption/desorption processes of radiocesium to/from sediment particles as forms of the labile and refractory fractions. The model reproduced the measured temporal changes of ^{137}Cs activities in surface sediment off Fukushima coastal waters, by normalization of the radiocsium transfer between seawater and sediment in relation to the particle diameter sizes. We found that the ^{137}Cs levels in sediment decreased more rapidly during the initial months after the accident, followed by a decrease of the labile fraction until the end of 2012. The apparent decrease of the total radiocesium level in surface sediments was estimated to occur at rates of approximately 0.2 y^{-1} within 20 km distance from the 1FNPP. The comparison of the decrease of ^{137}Cs concentrations in the demersal fish and the simulated labile fractions in sediment demonstrate that the consideration of ^{137}Cs transfer via sediment is essential for determining the radiocesium depuration mechanism in some demersal fish.

Declaration of competing interest

The authors declare that they have no known competing financial interests or personal relationships that could have appeared to influence the work reported in this paper.

Acknowledgments

This study was conducted mainly by the in-laboratory research fund of the Central research Institute of Electric Power Industry. A part of the measurement activity was funded by the Japan Society for the Promotion of Science KAKENHI Grant-in-Aid Research JP17K07895. The sediment sample collection from the sea-bed was carried out during the research cruise of Tokyo University of Marine Science and Technology. The stomach contents samples were supplied through the cooperation from TEPCO. We thank F. Taguchi (Denryoku Computing Center) for technical support.

Appendix A. Supplementary data

Supplementary data to this article can be found online at https://doi.org/10.1016/j.jenvrad.2020.106172.

References

Ambe, D., Kaeriyama, H., Shigenobu, Y., Fujimoto, K., Ono, T., Sawada, H., Saito, H., Miki, S., Setou, T., Morita, T., Watanabe, T., 2014. Five-minute resolved spatial distribution of radiocesium in sea sediment derived from the Fukushima Dai-ichi nuclear power plant. J. Environ. Radioact. 138, 264–275.

Aoyagi, K., Igarashi, S., 1999. On the size distribution of sediments in the coastal sea of Fukushima prefecture. Bull. Fukushima Pref. Fish. Exp. Stat. 8, 69–81 (in Japanese).

Bezhenar, R., Jung, K., Maderich, V., Willemsen, S., de With, G., Qiao, F., 2016. Transfer of radiocaesium from contaminated bottom sediments to marine organisms through benthic food chains in post-Fukushima and post-Chernobyl periods. Biogeosciences 13, 3021–3034.

Black, E., Buesseler, K., 2014. Spatial variability and the fate of cesium in coastal sediments near Fukushima, Japan. Biogeosciences 11, 5123–5137.

Cundy, A., Croudace, I., 1995. Physical and chemical association of radionuclides and trace metals in estuarine sediment: an example from Poole Harbour, Southern England. J. Environ. Radioact. 29, 191–211.

Fukuda, M., Aono, T., Yamazaki, S., Ishimaru, T., Kanda, J., Nishikawa, J., Otosaka, S., 2018. Factors controlling ^{134}Cs activity concentrations in sediment collected off the coast of Fukushima Prefecture in 2013–2015. Geochem. J. 52, 201–209.

Fukushima Prefecture, 2018. Results of environmental radioactivity monitoring by Fukushima prefecture (ports and sea surface fishing ground) (marine soil). Fukushima prefecture. https://emdb.jaea.go.jp/emdb/en/portals/1060207000/.

Fuller, A., Shawb, S., Wardc, M., Haigh, S., Mosselmans, F., Peacock, C., Stackhouse, S., Dent, A., Trivedi, D., Burke, I., 2015. Caesium incorporation and retention in illite interlayers. Appl. Clay Sci. 108, 128–134.

Ikenoue, T., Ishii, N., Kusakabe, M., Takata, H., 2018. Contribution of ^{137}Cs-enriched particles to radiocesium concentrations in seafloor sediment: reconnaissance experiment. PLoS One 13, e0204289. https://doi.org/10.1371/journal.pone.0204289.

Kusakabe, M., Oikawa, S., Takata, H., Misonoo, J., 2013. Spatiotemporal distributions of Fukushima-derived radionuclides in surface sediments in the waters off Miyagi, Fukushima, and Ibaraki prefectures, Japan. Biogeosciences 10, 5019–5030.

Ishimaru, T., Tateda, Y., Tsumune, D., Aoyama, M., Hamajima, Y., Kasamatsu, N., Yamada, M., Yoshimura, T., Mizuno, T., Kanda, J., 2019. Mechanism of radiocesium depuration in *Sebastes cheni* derived by simulation analysis of measured ^{137}Cs concentrations off southern Fukushima 2014-2016. J. Environ. Radioact. 203, 200–209.

Kusakabe, M., Inatomi, N., Takata, H., Ikenoue, T., 2017. Decline in radiocesium in seafloor sediments off Fukushima and nearby prefectures. J. Oceanogr. 73, 529–545.

Misumi, K., Tsumune, D., Tsubono, T., Tateda, Y., Aoyama, M., Kobayashi, T., Hirose, K., 2014. Factors controlling the spatiotemporal variation of ^{137}Cs in seabed sediment off the Fukushima coast: implications from numerical simulations. J. Environ. Radioact. 136, 218–228.

Nagao, S., Kanamori, M., Ochiai, S., Tomiara, S., Fukushi, K., Yamamoto, M., 2013. Export of ^{134}Cs and ^{137}Cs in the Fukushima river systems at heavy rains by typhoon Roke in september 2011. Biogeosciences 10, 6215–6223.

National Regulation Authority, 2019. Monitoring information of environmental radioactivity level. https://radioactivity.nsr.go.jp/en/list/205/list-1.html.

Otosaka, S., Kobayashi, T., 2013. Sedimentation and remobilization of radiocesium in the coastal area of Ibaraki, 70 km south of the Fukushima dai-ichi nuclear power plant. Environ. Monit. Assess. 185, 5419–5433.

Otosaka, S., Nakanishi, T., Suzuki, T., Satoh, Y., Narita, H., 2014. Vertical and Lateral transport of particulate radiocesium off Fukushima. Environ. Sci. Technol. 48, 12595–12602.

Otosaka, S., 2017. Processes affecting long-term changes in ^{137}Cs concentration in surface sediments off Fukushima. J. Oceanogr. 73, 559–570.

Ono, T., Ambe, D., Kaeriyama, H., Shigenobu, Y., Fujimoto, K., Sogame, K., Nishiura, N., Fujikawa, T., Morita, T., Watanabe, T., 2015. Concentration of ^{134}Cs + ^{137}Cs bonded to the organic fraction of sediments offshore Fukushima, Japan. Geochem. J. 49, 219–227.

Oughton, D., Borretzen, P., Salbu, B., Trnstad, E., 1997. Mobilization of ^{137}Cs and ^{90}Sr from sediment: potential source to arctic waters. Sci. Total Environ. 202, 155–165.

Perianez, R., 2008. A modelling study on ^{137}Cs and ^{239,240}Pu behaviour in the Alboran Sea, western Mediterranean. J. Environ. Radioact. 99, 694–715.

Rudjord, A., Oughton, D., Bergan, T., Christensen, G., 2001. Radionuclides in marine sediments- Distribution and processes. In: Palsson, S. (Ed.), Marine Radioecology. Final Reports from Sub-projects within the Nordic Nuclear Safety Research Project EKO-1, pp. 81–106. Roskilde, Denmark, 132 pp., ISBN 87-7893-056-1.

Shigenobu, Y., Ambe, D., Kaeriyama, H., Sohtome, T., Mizuno, T., Koshiishi, Y., Yamasaki, S., Ono, T., 2015. Investigation of radiocesium translation from contaminated sediment to benthic organisms. In: Nakata, K., Sugisaki, H. (Eds.), Impacts of the Fukushima Nuclear Accident on Fish and Fishing Grounds, vol. 252. Springer Japan, pp. 91–98.

Takata, H., Kusakabe, M., Inatomi, N., Hasegawa, K., Ikenoue, T., Watanabe, Y., Watabe, T., Suzuki, C., Misonoo, J., Morizono, S., 2017. Long-term distribution of radioactive cesium in the coastal seawater and sediments of Japan. Rep. Mar. Ecol. Res. Inst. 22 (Supplement), 17–25.

Tateda, T., Tsumune, D., Tsubono, T., Misumi, K., Yamada, M., Kanda, J., Ishimaru, T., 2016. Status of ^{137}Cs contamination in marine biota along the Pacific coast of eastern Japan derived from a dynamic biological model two years. J. Environ. Radioact. 151, 495–501.

Thornton, B., Ohnishi, S., Ura, T., Odano, N., Fujita, T., 2013. Continuous measurement of radionuclide distribution off Fukushima using a towed sea-bed gamma ray spectrometer. Deep Sea Res. Part I 79, 10–19.

Tokyo Electric Power Co, 2019. Analyzed result of radioactive substance near the Fukushima dai-ichi nuclear power plant. http://www.tepco.co.jp/decommission/data/analysis/index-j.html.

Tsumune, D., Tsubono, T., Aoyama, M., Hirose, K., 2012. Distribution of oceanic ^{137}Cs from the Fukushima Dai-ichi Nuclear Power Plant simulated numerically by a regional ocean model. J. Environ. Radioact. 111, 100–108.

Tsumune, D., Tsubono, T., Aoyama, M., Uematsu, M., Misumi, K., Maeda, Y., Yoshida, Y., Hayami, H., 2013. One-year, regional-scale simulation of ^{137}Cs radioactivity in the ocean following the Fukushima Dai-ichi Nuclear Power Plant accident. Biogeosciences 10, 5601–5617.

Wang, C., Baumann, Z., Madigan, D., Fisher, S., 2016. Contaminated marine sediments ss a source of cesium radioisotopes for benthic fauna near Fukushima. Environ. Sci. Technol. 50, 10448–10455.